Ferromagnetic copper-doped ZnO deposited on plastic substrates

2007 J. Phys.: Condens. Matter 19 236214

(http://iopscience.iop.org/0953-8984/19/23/236214)

IOP PUBLISHING JOURNAL OF PHYSICS: CONDENSED MATTER

J. Phys.: Condens. Matter **19** (2007) 236214 (11pp) doi:10.1088/0953-8984/19/23/236214

Ferromagnetic copper-doped ZnO deposited on plastic substrates

T S Herng[1], S P Lau[1,5], S F Yu[1], H Y Yang[1], K S Teng[2] and J S Chen[3,4]

[1] School of Electrical and Electronic Engineering, Nanyang Technological University, Nanyang Avenue, 639798, Singapore
[2] Multidisciplinary Nanotechnology Centre, School of Engineering, University of Wales Swansea, Singleton Park, Swansea SA2 8PP, UK
[3] Data Storage Institute, 5 Engineering Drive 1, 117608, Singapore
[4] Department of Material Science and Engineering, National University of Singapore, 119260, Singapore

E-mail: esplau@ntu.edu.sg

Received 9 March 2007, in final form 27 April 2007
Published 11 May 2007
Online at stacks.iop.org/JPhysCM/19/236214

Abstract

Copper-doped ZnO (ZnO:Cu) films with Cu content of up to 8.2 at.% were prepared by filtered cathodic vacuum arc technique on plastic substrates. The ZnO:Cu films with 1.3 at.% of Cu exhibited the highest saturated magnetic moment of 0.28 μ_B/Cu. The binding species of the Zn $2p_{3/2}$, and Cu $2p_{3/2}$ peaks are located at around 1022.1 and 933.6 eV respectively, as measured by x-ray photoelectron spectroscopy respectively. This implies that the Cu ions in the films are mainly in divalent states. The magnetic anisotropy of the ZnO:Cu samples under strain were also studied by bending the flexible samples into various directions. The results indicate that strain plays a role in the magnetic anisotropy of the ZnO:Cu films. The electrical transport and annealing measurements of the ZnO:Cu films suggested that Zn interstitial defects have a significant role in the observed ferromagnetism in the ZnO:Cu.

(Some figures in this article are in colour only in the electronic version)

1. Introduction

Diluted magnetic semiconductors (DMSs) are alloys where a stoichiometric fraction of the constituent atoms has been replaced by transition metal atoms [1]. Much of the attention of DMS materials is due to its potential application in spintronics, which exploit spin in magnetic materials along with the charge of electrons in semiconductors. There is increasing interest in ZnO-based DMSs because they become ferromagnetic when doped with most of the transition-metal elements and exhibit above-room-temperature (RT) ferromagnetism (FM). To date, most

[5] Author to whom any correspondence should be addressed.

DMS materials studied previously were deposited on solid substrates, such as Si and sapphire, due to high processing and preparation temperature,. Here we report a DMS material—Cu-doped ZnO (ZnO:Cu), which is capable of being deposited on plastic substrates and exhibits above-room-temperature FM. ZnO:Cu is predicted to be a half-metallic ferromagnet with 100% carrier polarization and a Curie temperature of 380 K by Ye *et al* on the basis of density functional calculations [2]. Unlike other transition-metal-doped ZnO (ZnO:TM; TM = Fe, Co, Ni, Mn) where the observed FM may relate to its secondary magnetic phases or metal precipitates, the non-magnetic phases of Cu, Cu_2O and CuO will make ZnO:Cu unambiguously an intrinsic DMS. In this paper, we investigate the magnetization of ZnO:Cu films deposited on plastic substrates subjected to various bending conditions and magnetic field directions. ZnO/polymer heterojunction light emitting diodes (LEDs) [3] and ZnO thin-film transistors [4] have been demonstrated using a processing temperature of $\sim$100 °C, which is comparable with large-area fabrication on plastic substrates. The demonstration of ferromagnetic and semiconducting ZnO:Cu thin films on a plastic substrate may facilitate the development of plastic spintronics.

2. Experiment

ZnO:Cu films were prepared on plastic (polycarbonate) substrates at RT using the filtered cathodic vacuum arc (FCVA) technique. The flexible and transparent polycarbonate substrates were chosen because of its high heat resistance and superior dimensional stability. The typical thickness of the polycarbonate substrate is 0.16 mm. Zn:Cu alloy targets containing 0.5, 1, 3, 5 and 7 at.% of Cu were used; the actual Cu content in the films was approximately 0.5, 1.3, 3, 4.4 and 8.2 at.%, respectively, as measured by x-ray photoelectron spectroscopy (XPS). The details of the FCVA apparatus have been described elsewhere [5]. The arc was operated in dc mode with a current of 60 A. The O_2 flow rate was maintained at 60 sccm. The typical thickness of the ZnO:Cu films were $\sim$220 nm. The roughness of the ZnO:Cu films is about 2 nm for a Cu concentration $\leqslant$4.4 at.% and 4 nm for a concentration $>$4.4 at.%, as determined by atomic force microscopy.

The magnetic properties of the ZnO:Cu films were investigated by an alternating gradient magnetometer (AGM) [6] with a maximum field of 10 kOe. To eliminate the spurious magnetic data, the ZnO:Cu samples and tweezers that were used were cleaned with acetone prior to magnetic measurement. The structural properties of the ZnO:Cu films on plastic substrates were studied by x-ray diffraction (XRD), scanning electron microscopy (SEM), high-resolution transmission electron microscopy (HRTEM) and selective area electron diffraction (SAED). Optical transmittance measurements of the ZnO:Cu were performed using a UV-2501PC spectrophotometer with a varying wavelength ranging from 200 to 1000 nm. Transport properties were investigated using the van der Pauw method in the temperature range from 300 down to 80 K.

3. Results and discussion

Figure 1 shows the XRD patterns of ZnO:Cu films prepared at RT on plastic substrates as a function of Cu concentration. The films exhibit predominately *c*-axis (002) texture at $\sim$34.3° corresponding to a ZnO wurtzite structure. The degradation of XRD intensity and its resolution are observed with increasing Cu concentration, indicating the increase in structural disorder of the ZnO:Cu films at higher Cu content. The incorporation of 3d transition ions generally deteriorates the crystallinity of ZnO, which is due to their low solubility and various valence states [7]. Within the sensitivity of XRD, no secondary phases were detected when the Cu

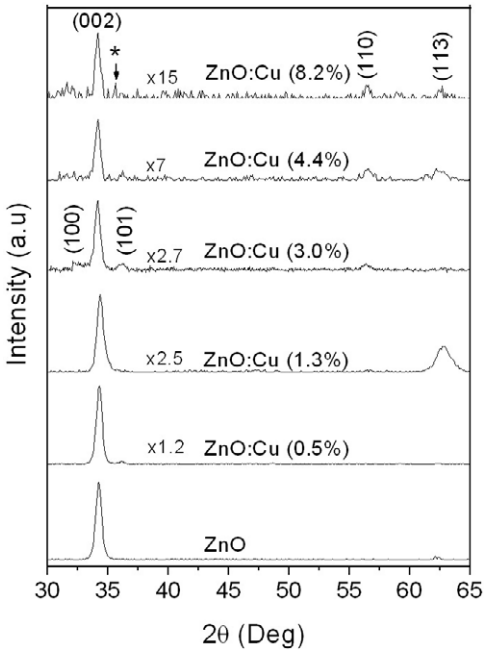

Figure 1. XRD spectra of the ZnO and ZnO:Cu films prepared at room temperature on plastic substrates. The weak intensity mark (*) indicates the presence of CuO phase.

concentration is $\leqslant$4.4 at.%. The appearance of the CuO phase in the structurally poor ZnO:Cu (8.2 at.%) is an indication that the solid solubility of Cu in ZnO has been exceeded.

The incorporation of Cu atoms into the lattice and their chemical bonding states were characterized by x-ray photoemission spectroscopy. The thin, insulating and flexible plastic has made XPS analysis unfavourable, thus ZnO:Cu films on silicon prepared under identical conditions with ZnO:Cu on plastic substrates were used in the XPS study. Figure 2 depicts XPS spectra of the Zn 2p, O 1s and Cu 2p core levels of the ZnO:Cu films. All the indexed peaks correspond to C, Cu, O and Zn; no foreign impurities are detected. The binding energy (BE) of Zn $2p_{3/2}$ states are centred at 1021.9 eV, as shown in figure 2(a), which corresponds to the BE of ZnO (1021.3–1022.2 eV) [8, 9]. The O 1s peaks are broad and asymmetric. It can be well fitted by two Gaussian curves, as shown in figure 2(b). The peak centred at 530.4 eV can be attributed to O–Zn bond formation, whereas the peak centred at 531.5 eV is associated with loosely bound oxygen (e.g. adsorbed O_2, –OH) chemisorbed on the surface. The Cu $2p_{3/2}$ peak appears at 933.4 eV, showing the Cu^{2+} ion state [12]. Apparently, the Cu $2p_{3/2}$ level shifts from 933.6 to 933.2 eV with increases in Cu concentration, as shown in figure 2(c). It has been suggested that metallic Cu^0($\sim$933 eV) [10] is likely to be formed at a Cu concentration of 8.2 at.%. In addition, the appearance of a peak (also known as a shake-up satellite) at around 9.8 eV above the main peak, as shown in figure 2(d), reveals the existence of the CuO phase [11] in ZnO:Cu (8.2 at.%). This is in good agreement with the XRD spectrum of ZnO:Cu (8.2 at.%), as illustrated in figure 1. In contrast, the ZnO:Cu (1.3 at.%) has a BE of 933.7 eV with no shake-up satellite peaks of Cu $2p_{3/2}$, indicating the presence of divalent Cu^{2+} ions in ZnO host material. More importantly, it is noted that the whole spectrum of the core level peaks of Zn 2p, Cu 2p and O 1s were shifted toward lower BE by $\sim$0.3 eV as the Cu concentration increases, implying that the valence band and its core levels band toward the Fermi level. The

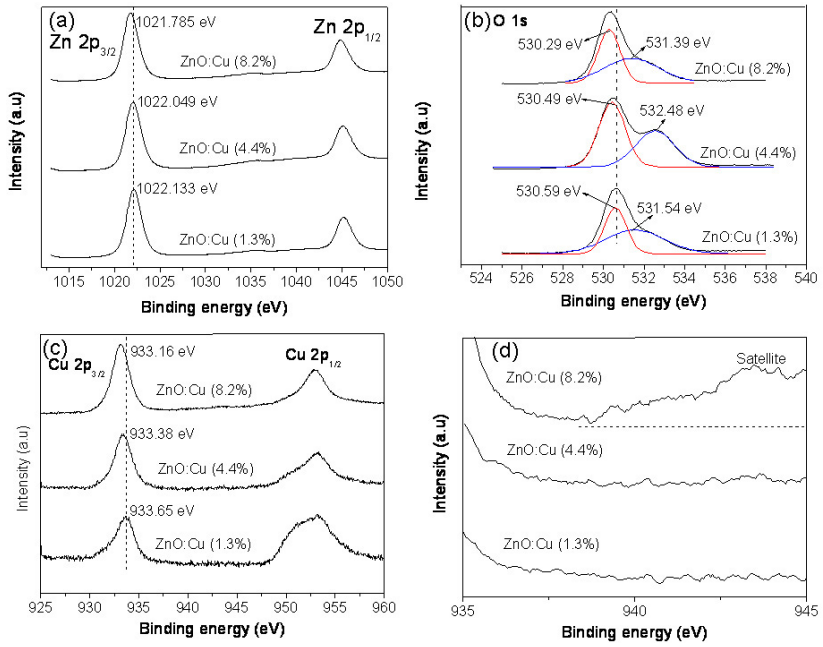

Figure 2. XPS spectra of (a) Zn 2p, (b) O 1s and (c) Cu 2p core level for the ZnO:Cu films. (d) The corresponding satellite peak of Cu 2p in the ZnO:Cu films.

observed shift in BE toward lower energy typically suggests an upward band bending of the energy core levels. In this case, the BE shift indicates a change in the electronic properties in the ZnO:Cu film, such as the film becoming more p-type as the Cu concentration increases, and this is due to Cu being a potential hole dopant for ZnO, as suggested by others [12, 13].

The typical magnetization curves of ZnO:Cu (1.3 at.%) films prepared on plastic substrates with applied fields parallel and perpendicular to the sample are shown in figure 3(a). Well-defined hysteresis loops with a coercivity (H_c) of about 90 Oe are observed from the sample, as shown in the insets of figure 3(a). The sample exhibits no magnetic anisotropy in the high-magnetic-field region (10 kOe), but an 'easy-plane' ferromagnetism is apparent at low field (<2 kOe) with a field perpendicular to the sample, as shown in the inset of figure 3(a). As proposed by Sati *et al*, the easy-plane ferromagnetism in ZnO:Cu may be considered as a signature of intrinsic ferromagnetism, where Cu^{2+} ions in ZnO possess a strong single-ion anisotropy [14]. Chanier *et al* reported the tetrahedral and trigonal crystal field of ZnO together with spin-orbit coupling that leads to a magnetic anisotropy [15]. However, further experiments are needed to confirm the existence of strong single-ion anisotropy in ZnO:Cu films.

As shown in figure 3(b), RT ferromagnetism is observed from samples with Cu content up to 4.4 at.%. The ZnO:Cu (1.3 at.%) film exhibits the strongest magnetic ordering with a saturated magnetic moment (M_s) of 0.28 μ_B/Cu among all other samples. Since the ZnO:Cu (1.3 at.%) exhibited the strongest magnetic moment, this sample has been characterized in greater detail and will be discussed later. The H_c and M_s reduce with an increase in Cu content. The M_s reduces significantly to 0.072 μ_B/Cu for Cu content of 3.0 at.%. This appears that an increase in lattice disorder at high Cu content degrades the magnetic properties of the ZnO:Cu films. Paramagnetism is observed in ZnO:Cu (8.2 at.%) which may be attributed to the formation of anti-ferromagnetic CuO phases [16] and its poor crystallinity. It is worthwhile

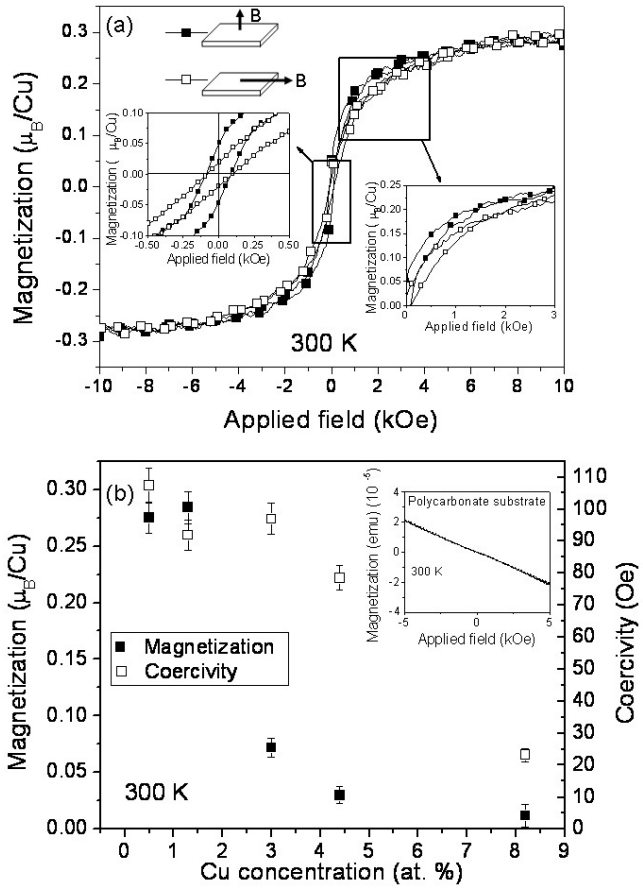

Figure 3. (a) Magnetization versus H curve of ZnO:Cu (1.3 at.%) film on plastic substrates at 300 K. The insets show the magnified magnetization versus H curve at two different low applied field regions. (b) Saturated magnetization and coercivity as a function of Cu concentration. The in-plane M–H curves of polycarbonate substrate measured at 300 K is shown in the inset of (b).

highlighting that the diamagnetic background of the substrate has been subtracted from all the magnetization data shown here. No magnetic ordering could be detected in the plastic substrate, confirming that the plastic substrate is not responsible for the observed FM in the samples, as illustrated in the inset of figure 3(b). In addition, there is no trace of magnetism in the undoped ZnO film. It is noted that the observed M_s of ZnO:Cu films on plastic substrates are compatible to other ZnO-based DMSs on Si and sapphire substrates [17]. Furthermore, the ZnO:Cu films exhibit RT ferromagnetism without being co-doped with other transition-metal elements (such as Fe or Mn) [18] or N [19]. The M_s of ZnO:Cu (1.3 at.%) on plastic substrate was weakened by 30% compared with the sample prepared on Si substrate ($M_s \sim 0.4\ \mu_B$/Cu) under identical growth conditions. The relatively low M_s of the ZnO:Cu on plastic substrate could be attributed to the relatively poor crystal quality of the sample compared to that prepared on Si.

One of the most remarkable aspects of ZnO:Cu on plastic substrates is its flexibility. Since the ZnO:Cu films can be bent into various shapes, it may be useful for the study of magnetic properties under strain conditions. The ZnO:Cu samples were bent to about 40° from the base plane with a radius of curvature of 5.7 mm using a non-magnetic 'C' shaped plastic tube

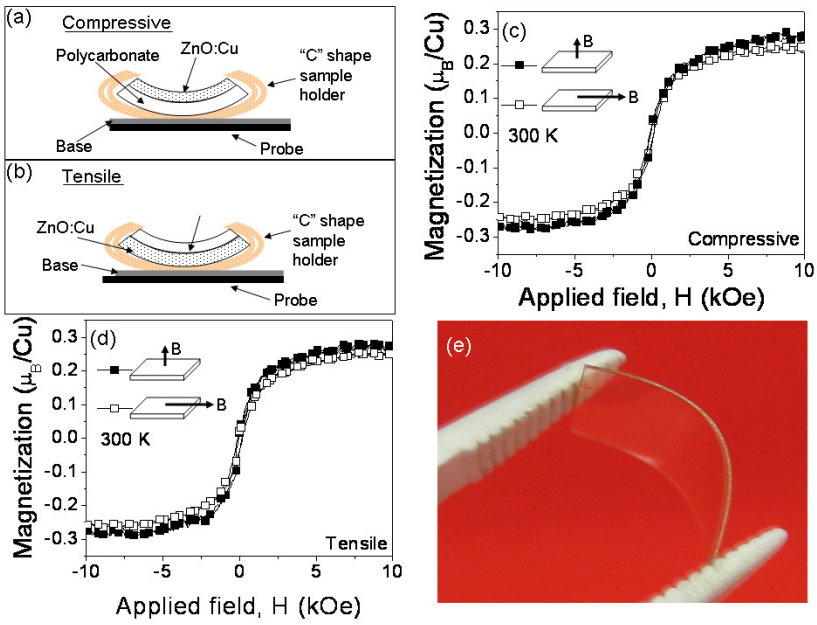

Figure 4. Schematic diagrams of ZnO:Cu films under (a) compressive and (b) tensile stress. Magnetic properties of ZnO:Cu (1.3 at.%) under (c) compressive stress and (d) tensile stress with external magnetic fields applied parallel and perpendicular to the samples. (e) Photograph of ZnO:Cu on plastic substrate under strain.

Table 1. The saturated magnetic moment of the ZnO:Cu (1.3%) under various bending conditions with a magnetic field of 10 kOe applied parallel and perpendicular to the film.

Applied magnetic field direction	Flat (emu cm^{-3})	Compressive (emu cm^{-3})	Tensile (emu cm^{-3})
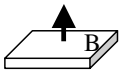	0.28	0.26	0.27
	0.28	0.24	0.26

as a holder. The magnetic anisotropy of the samples under compressive (inward bending) and tensile (outward bending) stress were studied. The schematic diagrams of the ZnO:Cu films under compressive and tensile stresses are shown in figures 4(a) and (b), respectively. Figures 4(c) and (d) show the magnetization curves of the ZnO:Cu (1.3 at.%) films under compressive and tensile stresses with an M_s of 0.24 μ_B/Cu and 0.26 μ_B/Cu, respectively. The M_s of the ZnO:Cu (1.3 at.%) at an applied field of 10 kOe under strain conditions is tabulated in table 1. It is recalled that no magnetic anisotropy in the flat ZnO:Cu sample can be observed at the applied field of 10 kOe. However, the magnetic anisotropy at high applied field becomes apparent for the samples under strain conditions. For the compressively stressed sample, the M_s can be different by ∼8% when the field is applied parallel and perpendicular to the sample. In addition, the M_s of the sample can be reduced by 15% when compared with the flat sample under parallel field. The observed magnetic anisotropy of the stressed samples can be attributed to strain in the ZnO:Cu films. The internal strain could lead to lattice distortion and produce

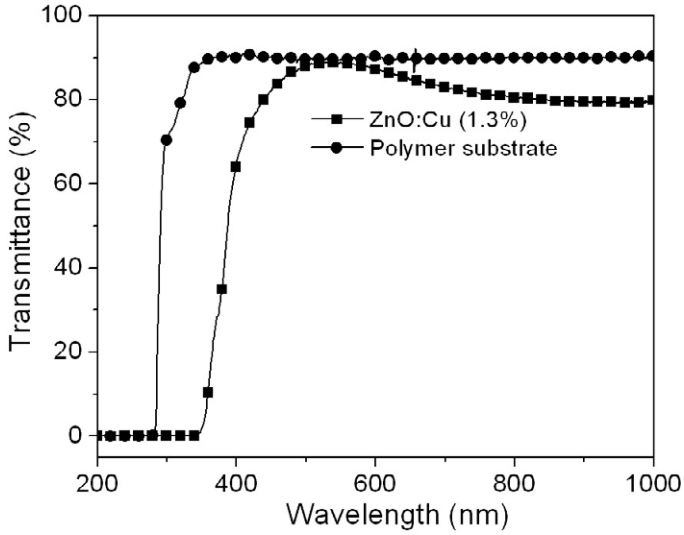

Figure 5. Optical transmission spectra of ZnO:Cu (1.3 at.%) and the polycarbonate substrate. The baseline was measured in air, and the reference was also measured in air, in order to quantify the total amount of transmitted light.

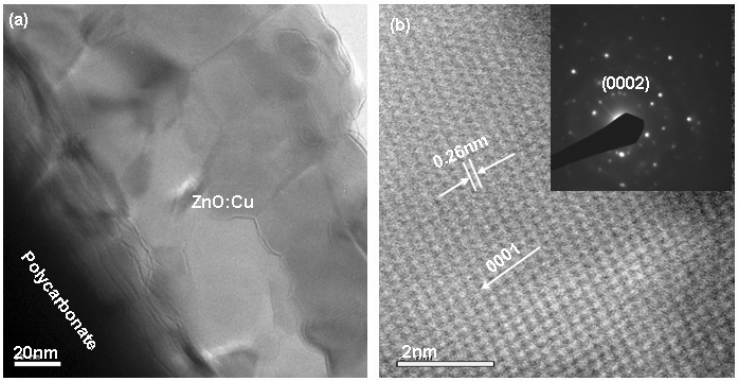

Figure 6. (a) TEM image at the interface of ZnO:Cu (1.3 at.%) film and plastic substrate. (b) HRTEM image of ZnO:Cu (1.3 at.%) on plastic substrate showing (002) planes with the lattice spacing of 0.26 nm and its corresponding SAED pattern.

magneto-elastic-driven anisotropy. The results indicate that strain plays a role in the magnetic anisotropy of the ZnO:Cu films.

The photograph in figure 4(e) shows the fully transparent ZnO:Cu (1.3 at.%) on plastic substrate at bending condition. The average transmittance of ZnO:Cu (1.3 at.%) is ∼82% in the visible region, as shown in figure 5. High-resolution transmission electron microscopy (HRTEM) studies were carried out to ascertain the microscopic homogeneity of the ZnO:Cu films. Figure 6(a) reveals that the interface between the ZnO:Cu (1.3 at.%) film and the plastic substrate is smooth and abrupt. It appears that there is no interface distortion or impurity at the interface. Taking together the weak magnetic anisotropy and TEM images, it is reasonable to rule out the possibility of localized interface defects which could lead to the observed FM [20].

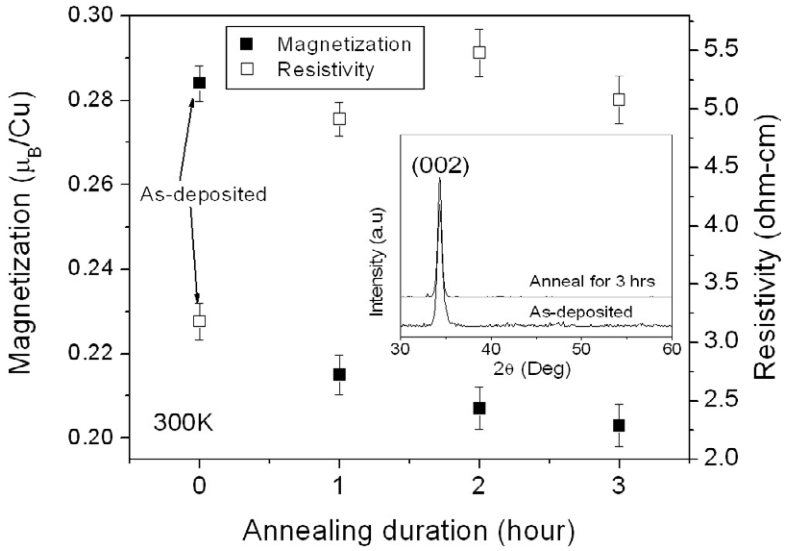

Figure 7. Variation of saturated magnetic moment and resistivity of ZnO:Cu (1.3 at.%) film annealed at 100 °C for various times in vacuum ambient. Inset: XRD spectra of the as-deposited and annealed ZnO:Cu (1.3 at.%) films.

A well-oriented (0002) plane of ZnO:Cu (1.3 at.%) with an interplanar distance of 0.26 nm is shown in figure 6(b). There are no detectable traces of any secondary phases or clusters of any ferromagnetic oxide or Cu-related precipitates, indicating good crystallinity and homogeneity of the sample. The inset of figure 6(b) shows the selected area electron diffraction (SAED) pattern of the ZnO:Cu, which reflects the polycrystalline structure.

In order to study the stability of FM in the ZnO:Cu on plastic substrates, low-temperature (∼100 °C) annealing for 1–3 h in vacuum was carried out. A low annealing temperature of 100 °C is crucial to ensure that there is no plastic deformation in the substrate. The polycarbonate substrate retained its diamagnetism after annealing at 100 °C. The M_s of the annealed ZnO:Cu (1.3 at.%) reduces to 0.20 μ_B/Cu (∼29% reduction) after 3 h of annealing, as illustrated in figure 7. The gradual reduction of magnetic properties is further explored by structural and electrical studies on the annealed ZnO:Cu films. XRD reveals no obvious changes in the structural properties of the as-deposited and annealed samples (3 h), as shown in the inset of figure 7. The influence of structural defects or disorder toward FM is trivial under a low annealing temperature. On the other hand, the resistivity of the ZnO:Cu films increases slightly with annealing time. The electron concentration of the samples is reduced to 4.2×10^{16} cm^{-3}, 3.1×10^{16} cm^{-3} and 1.7×10^{16} cm^{-3} after being annealed for 1 h, 2 h and 3 h, respectively. The above results suggest that the resistivity, carrier concentration and magnetic moment are correlated. The gradual decrement of carrier concentration with annealing duration may be attributed to out-diffusion of shallow donor defects such as a zinc interstitial (Zn_i) to the second-nearest-neighbour position. Zn_i is the most mobile defect among the native defects in the ZnO system; it has a relatively high self-diffusivity coefficient, even down to 90 K [21]. The Zn_i defect has low diffusion barriers and can easily diffuse into the lattice at a relatively low temperature compared with other defects [22]. Density functional theory calculations suggested that Zn_i plays a vital role in inducing the FM, so the reduction of Zn_i would lead to the degradation of magnetic ordering [23]. Recently, it has been reported

that FM can be enhanced by introducing Zn_i defects into ZnO DMS [24, 25]. Wang *et al* reported that Zn_i is the dominant defect in ZnO films prepared by the filtered cathodic vacuum arc technique at RT [5]. The energetic Zn ions produced by the cathodic arc at a low substrate temperature favoured the formation of Zn_i in the ZnO films. Since our ZnO:Cu films were deposited at RT with similar growth conditions to the previously reported ZnO films, a large concentration of Zn_i should be present in our samples. Ye *et al* reported that FM in ZnO:Cu is not related to hole mediation but to Zn_i, and the presence of oxygen vacancies would weaken the FM [2]. Thus the oxygen vacancy is unlikely to be the cause of the reduced M_s in our samples after annealing.

Now let us consider the relationship between the magnetic and electrical properties of the ZnO:Cu (1.3 at.%). In order to circumvent the poor adhesion of the contact layer and the loose contact between the probe and the ZnO:Cu films on plastics substrates at low temperature, the electrical analysis was carried out on ZnO:Cu films deposited on quartz substrates. The electrical analysis of the ZnO:Cu films on quartz should give a relatively good representation of its counterpart on plastic substrate, as it is found that the magnetic and electrical variations in both films were less than 13% at RT. Figure 8(a) shows the temperature dependence of electrical conductivity (σ) on undoped ZnO and ZnO:Cu films. The σ increases with temperature, where ZnO and ZnO:Cu films exhibit metallic and semiconductor behaviour, respectively. For a temperature between 200 and 300 K, the conductivity gives a linear Arrhenius plot, indicating band conduction of carrier electrons [26]. The activation energies (E_a) of the undoped ZnO, ZnO:Cu (0.5 at.%) and ZnO:Cu (1.3 at.%) were determined to be 0.45 meV, 7.32 meV and 28 meV, respectively, in the temperature range between 200 and 300 K. The increase in E_a is due to the decrement of the carrier concentration with increasing Cu content. This is because Cu introduces a deep acceptor level and it traps electrons from the conduction band [27]. As is evident, Hall effect measurements depict that the undoped ZnO, ZnO:Cu (0.5 at.%) and ZnO:Cu (1.3 at.%) exhibited electron concentrations of 8.04×10^{19} cm^{-3}, 2.42×10^{18} cm^{-3} and 7.2×10^{16} cm^{-3} at RT, respectively. The result is corroborated by the observed upward band bending of the core levels with increasing Cu concentration. Indeed, the E_a value ($\sim$28 meV) is in good agreement with the Zn_i empirical activation level, as observed by Natsume *et al* [26]. However, the conductivity of the ZnO:Cu deviates from the Arrhenius plot at temperatures lower than 200 K. Hence, the data were re-plotted and it is evident that the $\ln(\sigma)$ is linear as a function of $T^{-1/2}$ for temperatures below 200 K, as illustrated in figure 8(b). The linearity of $\ln(\sigma)$ versus $T^{-1/2}$ is qualitatively consistent with the prediction of magnetic polaron (MP) variable range hopping (VRH) in the presence of electron–electron interaction [28]. The VRH mechanism provides a reasonable explanation of transport behaviour in magnetic semiconductors and has been applied to model the magnetoresistance (MR) observed in DMS. Indeed, MR in ZnO:Cu films has been observed at temperatures ranging from 5 to 300 K [29]. The existence of MP in the ZnO:Cu films may shed light on the ferromagnetism mechanism to be discussed next. In addition, the conductivity and carrier concentration of the ZnO:Cu (0.5 at.%) may be sufficient to be used as a spin-injection layer for spin-LEDs and spin-transistors.

It is noteworthy that the low carrier concentration in the ZnO:Cu films (an electron concentration $\sim 10^{16}$ cm^{-3}) may not link to a carrier-mediated mechanism such as double exchange or an Ruderman–Kittel–Kasuya–Yosida (RKKY) mechanism. The FM of ZnO:Cu prepared at RT is proposed to be invoked by a super coupling mechanism based on the bound magnetic polaron (BMP) model [30]. Shallow donors of Zn_i are located throughout the lattice at arbitrary distances with respect to Cu^{2+} sites. We expect that $Cu^{2+}\square Cu^{2+}$ groups will be common in the structure, where $\square$ denotes a Zn_i. The shallow donor state of Zn_i defects [31] occupies an orbital and overlaps the d shells of both Cu ions; this constitutes BMP

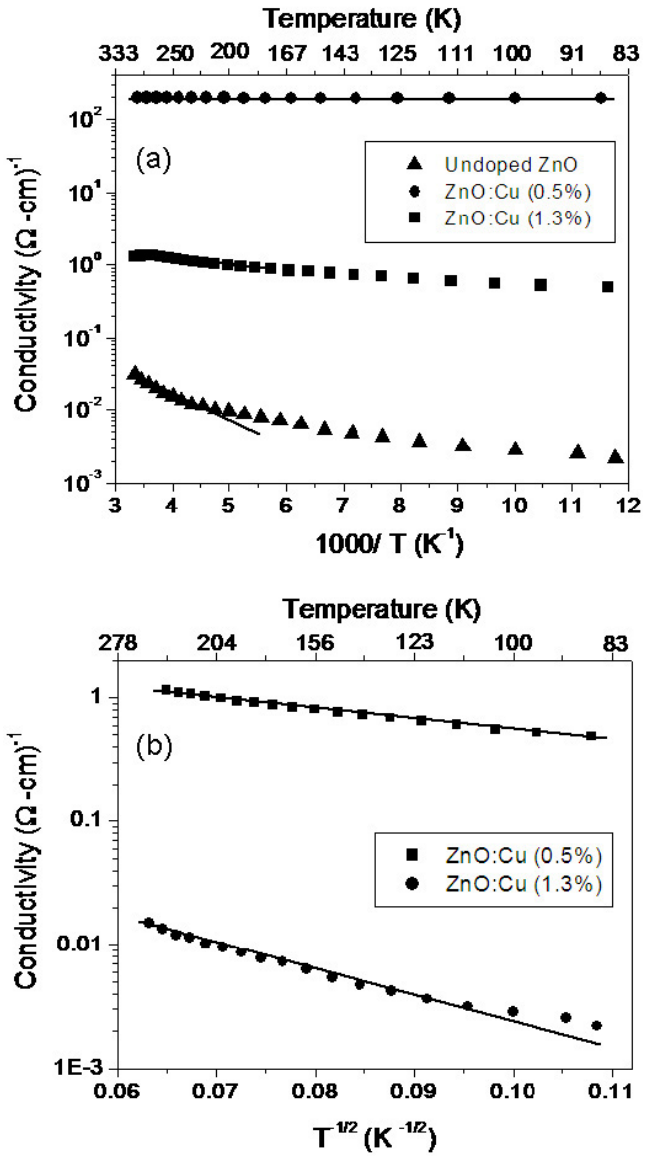

Figure 8. (a) Arrhenius plots of conductivity of ZnO, ZnO:Cu (0.5 at.%) and ZnO:Cu (1.3 at.%). (b) The plot of $\ln(\sigma)$ as a function of $T^{-1/2}$ for ZnO:Cu (0.5 at.%) and ZnO:Cu (1.3 at.%).

formation [30]. Based on the BMP model, the magnetic properties of the ZnO:Cu films could be tuned through Cu and defect concentrations, which are in good agreement with our results.

4. Conclusion

In conclusion, we have demonstrated RT ferromagnetism in flexible and transparent ZnO:Cu films on plastic substrates. The ZnO:Cu (1.3 at.%) film exhibited a saturated magnetic moment of 0.28 μ_B/Cu. The annealing experiment showed that the observed FM is not linked to

oxygen vacancies but the presence of Zn_i, which plays a crucial role in mediating the FM in the ZnO:Cu films. The magnetic and transport properties of the ZnO:Cu films are consistent with the BMP model for the observed ferromagnetism. The realization of unambiguous and tunable ferromagnetic properties of ZnO:Cu on plastic substrates may open up new prospects for plastic spintronics such as spin-LEDs and spin–transistors.

Acknowledgments

This work was partially supported by a Ministry of Education grant ARC 02/06. One of the authors (HYY) acknowledges the support of Singapore Millennium Foundation Fellowships.

References

[1] Ohno H 1998 *Science* **281** 951
[2] Ye L-H, Freeman A J and Delley B 2006 *Phys. Rev.* B **73** 033203
[3] Konenkamp R, Word R C and Godinez M 2005 *Nano Lett.* **5** 2005
[4] Carcia P F, McLean R S, Reilly M H and Nunes G Jr 2003 *Appl. Phys. Lett.* **82** 1117
[5] Wang Y G, Lau S P, Lee H W, Yu S F, Tay B K, Zhang X H, Tse K Y and Hng H H 2003 *J. Appl. Phys.* **94** 1597
[6] Flanders P J 1988 *J. Appl. Phys.* **63** 3940
[7] Jimenez-Gonzalez A E 1997 *J. Solid State Chem.* **128** 176
[8] Grohmann I, Peplinski B and Unger W 1992 *Surf. Interface Anal.* **19** 591
[9] Wagner C D, Riggs W M, Davis L E, Moulder J F and Muilenberg G E 1979 *Handbook of X-ray Photoelectron Spectroscopy* (Eden Prairie, MN: Perkin Elmer)
[10] Chastain J and King R C Jr 1995 *Handbook of X-ray Photoelectron Spectroscopy* (Eden Prairie, MN: Physical Electronics)
[11] Scrocco M 1979 *Chem. Phys. Lett.* **63** 52
[12] Fons P, Nakahara K, Yamada A, Iwata K, Matsubara K, Takasu H and Niki S 2002 *Phys. Status Solidi* b **229** 849
[13] Lee H J, Kim B S, Cho C R and Jeong S Y 2004 *Phys. Status Solidi* b **241** 1533
[14] Sati P, Hayn R, Kuzian R, Regnier S, Schafer S, Stepanov A, Morhain C, Deparis C, Laugt M, Goiran M and Golacki Z 2006 *Phys. Rev. Lett.* **96** 017203
[15] Chanier T, Sargolzaei M, Opahle I, Hayn R and Koepernik K 2006 *Phys. Rev.* B **73** 134418
[16] Brumage W H, Dorman C F and Quade C R 2001 *Phys. Rev.* B **63** 104411
[17] Liu C, Yun F and Morkoc H 2005 *J. Mater. Sci.* **16** 555
[18] Hong N H, Brize V and Sakai J 2005 *Appl. Phys. Lett.* **86** 082505
[19] Buchholz D B, Chang R P H, Song J H and Ketterson J B 2005 *Appl. Phys. Lett.* **87** 082504
[20] Coey J M D 2005 *J. Appl. Phys.* **97** 1
[21] Erhart P and Albe K 2006 *Appl. Phys. Lett.* **88** 201918
[22] Kohan A F, Ceder G, Morgan D and van de Walle C G 2000 *Phys. Rev.* B **61** 15019
[23] Sluiter M H F, Kawazoe Y, Sharma P, Inoue A, Raju A R, Rout C and Waghmare U V 2005 *Phys. Rev. Lett.* **94** 187204
[24] Schwanz D A and Gamelin D R 2004 *Adv. Mater.* **16** 2115
[25] Khare N, Kappers M J, Wei M, Blamire M G and MacManus-Driscoll J L 2006 *Adv. Mater.* **18** 1449
[26] Natsume Y, Sakata H, Hirayama T and Yanagida H 1992 *J. Appl. Phys.* **72** 4203
[27] Pearton S J, Norton D P, Ip K, Heo Y W and Steiner T 2004 *J. Vac. Sci. Technol.* B **22** 932
[28] Foygel M, Morris R D and Petukhov A G 2003 *Phys. Rev.* B **67** 134205
[29] Rao K V 2007 private communication
[30] Coey J M D, Venkatesan M and Fitzgerald C B 2005 *Nat. Mater.* **4** 173
[31] Look D C, Farlow G C, Reunchan P, Limpijumnong S, Zhang S B and Nordlund K 2005 *Phys. Rev. Lett.* **95** 225502